4-2010

Efficient simulation of non-linear effects in 2D optical nanostructures to TM waves

Alexander V. Kildishev
Birck Nanotechnology Center, School of ECE, kildishev@purdue.edu

Natalia M. Litchinitser
SUNY Buffalo

Kildishev, Alexander V. and Litchinitser, Natalia M., "Efficient simulation of non-linear effects in 2D optical nanostructures to TM waves" (2010). *Birck and NCN Publications.* Paper 692.
http://dx.doi.org/10.1016/j.optcom.2009.09.039

Optics Communications 283 (2010) 1628–1632

Contents lists available at ScienceDirect

Optics Communications

journal homepage: www.elsevier.com/locate/optcom

Invited paper

Efficient simulation of non-linear effects in 2D optical nanostructures to TM waves

Alexander V. Kildishev [a,*], Natalia M. Litchinitser [b]

[a] Birck Nanotechnology Center, Purdue University, 1205 West State Street, West Lafayette, IN 47907, USA
[b] Department of Electrical Engineering, The State University of New York at Buffalo, Buffalo, NY 14260, USA

ARTICLE INFO

Article history:
Received 1 September 2009
Received in revised form 17 September 2009
Accepted 17 September 2009

ABSTRACT

We develop a theory to study stationary TM-type waves propagating in a nanostructured layer of 2D non-linear optical metamaterial or plasmonic device. It is assumed that the layer is inhomogeneous and contains non-linear isotropic elemental materials with non-linearity and loss mechanisms, including both linear and non-linear losses. While modeling of the non-linear propagation of the TE-type scalar waves is straightforward, the TM-type waves within the standard *E*-field formulations of non-linear optics cannot be treated in a purely scalar *H*-field context since an implicit equation for the non-linear dielectric functions should be resolved otherwise. A new formulation, which is built on the solution of the implicit equation for the non-linear dielectric function, is proposed. We use a general cubic non-linearity to illustrate all of the important features of the proposed approach. The general solution for scalar *H*-field waves is validated versus our previously tested particular cases, and important differences are shown between those cases and the general solution. These details, for example, include the link between linear and non-linear loss mechanisms, and connection between the linear and non-linear dielectric functions. The proposed approach is used for modeling a non-linear focusing device with optically controlled isotropic Kerr-type non-linearity; the simulation results prove the predicted functioning of the device.

1. Introduction

Negative index of refraction, antiparallel phase and energy velocities, magnetism in optics, backward phase-matched non-linear wave interactions, and cloaking are just few examples of the fascinating phenomena enabled by metamaterial technology. Due to the complexity of metamaterial structures, the realization of all these remarkable properties and their potential applications would not have been possible without the availability of advanced and specialized numerical modeling tools. Therefore, numerical analysis quickly becomes an essential component of metamaterial research. (Difficulties of the finite element electromagnetic analysis of the metamaterials with extreme linear parameters have been discussed for example in Refs. [1,2].)

While several advanced numerical tools for the design and optimization of nanostructured linear metamaterials were recently developed, accurate numerical modeling of non-linear metamaterials remains challenging. A majority of theoretical and numerical studies to date treat non-linear metamaterials as uniform media with effective dielectric permittivity and magnetic permeability; i.e., the effects induced by the actual nanostructure, such as local field enhancement, are not taken into account. Therefore, efficient and reliable numerical modeling tools that take into account fine structural and electromagnetic properties are essential for developing future applications of optical metamaterials and plasmonic devices for nanophotonics.

Currently, plasmonic nanostructures can be designed and manufactured in a wide range of geometries, including single- and double-periodic arrays of identical (and often coupled) resonant elements such as silver or gold strips, nanorods and elliptic cylinders, which define the design properties and functionality [3,4].

The simplest single-period arrays of 2D plasmonic elements (e.g., very long, 'infinite', silver or gold strips or wires) in layered structures are of broad interest for nanoscale non-linear devices because of their more robust design and fabrication simplicity [4]. With the magnetic field aligned along their largest (infinite) dimension such structures are capable of producing symmetric (electric) and asymmetric (magnetic) modes depending on a given geometry. Arranging nanostructured plasmonic elements with complementary non-linear materials, nanoscale optical metamaterials can be designed with properties that make them applicable to optoelectronic devices, biomedical applications, and sensing.

Even these simplest structures present a significant challenge for their efficient numerical simulation and optimization in order to enhance non-linear performance and achieve a required functionality. Examples of such structures include aligned gold strip antennae and sandwiched silver nanostrips [4], which are known to exhibit localized surface plasmon resonances and could be useful for optical limiting and non-linearly-tunable photonic devices.

* Corresponding author.
E-mail address: kildishev@purdue.edu (A.V. Kildishev).

0030-4018/$ - see front matter © 2009 Elsevier B.V. All rights reserved.
doi:10.1016/j.optcom.2009.09.039

In addition to the general simulation complexity, the non-linear effects normally depend on the magnitude of the *E*-field strength vector, $|\vec{E}|$, and thus cannot be straightforwardly introduced in a scalar *H*-field formulation. This requires that a set of fully vectorial 3D equations must be solved. Moreover, photomodification and light-induced damage of optical metamaterials and other nanostructures made of 2D plasmonic elements embedded in a non-linear host calls for a multiphysics simulation environment. Multiphysics involves simulations that combine multiple interconnected physical phenomena through solving coupled systems of partial differential equations. Thus, the multiphysics simulation environment for photomodification modeling should include elastic and thermal effects treated coherently with the propagation of electromagnetic waves. These simulation requirements necessitate enhanced simulation efficiency and every effort should be taken to fully exploit the possibility of using simpler purely scalar wave equations.

We have already demonstrated a related method for a simplified efficient analysis of nonlinearities in optical nanostructures with scalar *H*-field frequency-domain formulation (TM-type waves) [5]. The approach was limited to the basic case of lossless linear susceptibility ($\mathrm{Re}(\chi^{(1)}) > 1$, $\mathrm{Im}(\chi^{(1)}) = 0$) and either purely real or purely imaginary cubic susceptibility; it was shown to produce fast and accurate results without superfluous vector *E*-field formalism.

In this paper, a novel general approach for the efficient simulation of non-linear wave interactions in optical nanostructured materials, including metamaterials and photonic devices is discussed. The approach exploits purely scalar monochromatic *H*-field formulation, in contrast to a standard TM-wave representation using an *E*-field dependent non-linear susceptibility.

2. Method

We first consider the propagation of a monochromatic wave of frequency ω (time-dependent term $e^{-i\omega t}$ is omitted). Furthermore, since many optically non-linear materials are anisotropic and demand the use of tensors to describe their material properties, we use appropriate tensors for at least the most general, initial 2D and 3D formulations.

The electric displacement vector, $\vec{D}(\vec{E})$ in a medium with a non-linear local dielectric susceptibility tensor $\boldsymbol{\chi}(\vec{E})$ is given by

$$\vec{D} = (\boldsymbol{\varepsilon}_l + \boldsymbol{\chi}(\vec{E}))\vec{E}, \tag{1}$$

here $\boldsymbol{\varepsilon}_l$ is the linear part of the local dielectric function (an anisotropic tensor in general), and $\vec{E}$ is the *E*-field strength vector. We may also consider an inverse function $\boldsymbol{\varepsilon}^{-1}(\vec{D})$

$$\vec{E} = \boldsymbol{\varepsilon}^{-1}(\vec{D})\vec{D}, \tag{2}$$

where $\boldsymbol{\varepsilon}^{-1}$ is the inverse of the local dielectric function. Then combining (1) and (2) in a matrix equation we arrive at:

$$\boldsymbol{\varepsilon}^{-1} = \left[\boldsymbol{\varepsilon}_l + \boldsymbol{\chi}(\boldsymbol{\varepsilon}^{-1}\vec{D})\right]^{-1}. \tag{3}$$

Since the displacement vector components are connected to $\vec{H}$ through the curl equation

$$\vec{D} = i\omega^{-1}\nabla \times \vec{H}, \tag{4}$$

substituting (4) into (3) yields an implicit form,

$$\boldsymbol{\varepsilon} = \boldsymbol{\varepsilon}_l + \boldsymbol{\chi}(i\omega^{-1}\boldsymbol{\varepsilon}^{-1}\nabla \times \vec{H}), \tag{5}$$

Eq. (5) allows to compute the inverted tensor $\boldsymbol{\varepsilon}^{-1}$ through a known non-linear susceptibility function $\boldsymbol{\chi}$, but it substantially restrains any standard numerical frequency-domain 2D simulation scheme built on a scalar *H*-field wave equation with non-linear effects.

Indeed, in a frequency-domain formulation for TM-type waves and a 2D geometry, a single scalar wave equation

$$\nabla \cdot (\boldsymbol{\varepsilon}^{-1}\nabla h) + \omega^2\mu_0 h = 0, \tag{6}$$

can be used for the out-of-plane field component, $\vec{H} = \hat{\mathbf{z}}h(x, y; \omega)$. For TE modes, where only scalar *E*-field is employed, incorporating the non-linearity (1) is quite simple. However, for TM modes, which are relevant for many resonant plasmonic structures, it would be imperative to have (5) solved along with the solution of (6). This problem is not an issue in a 3D *E*-field based frequency-domain formulation. But then again, 3D methods exhibit significant redundant complexity compared with the scalar frequency-domain formulation of 2D geometries and are substantially less efficient for computationally expensive problems. This is especially true for multiphysics content, where coupled non-linear phenomena should be solved consistently. In order to circumvent this redundancy, we solve the resulting cubic Eq. (4) for $\boldsymbol{\varepsilon}$ in terms of the *H*-field and a given $\boldsymbol{\chi}^{(3)}$. For TM waves, Eq. (5) can be simplified

$$\boldsymbol{\varepsilon} = \boldsymbol{\varepsilon}_l + \boldsymbol{\chi}\Big(i(\omega|\boldsymbol{\varepsilon}|)^{-1}\Big[(\varepsilon_{yy}h^{(y)} + \varepsilon_{xy}h^{(x)})\hat{\mathbf{x}} - (\varepsilon_{yx}h^{(y)} + \varepsilon_{xx}h^{(x)})\hat{\mathbf{y}}\Big]\Big), \tag{7}$$

which, provided that the medium is isotropic (and $\boldsymbol{\varepsilon}$, $\boldsymbol{\varepsilon}_l$, and $\boldsymbol{\chi}$ are just scalars, ε, ε_l, and χ), can be further simplified in the following manner,

$$\varepsilon = \varepsilon_l + \chi(i(\omega\varepsilon)^{-1}[\hat{\mathbf{x}}h^{(y)} - \hat{\mathbf{y}}h^{(x)}]). \tag{8}$$

Thus far, this section has shown a (seemingly) simple matrix Eq. (5) describing a very general optical non-linearity without specifying its exact physical origin or detailing a specific physical effect. The section shows how the anisotropic dielectric function can be determined through a given non-linear susceptibility function χ and the gradients of the applied magnetic field in an optically non-linear medium. Next, we validate the proposed treatment of optical non-linearities with a realistic yet relatively simple non-linear saturation effect; we also show our recent simplified mathematical formulations for cubic nonlinearities [5] that relate the polarization to the spatial derivatives of the magnetic field.

3. Cubic nonlinearities in 2D nanostructures

3.1. A general cubic non-linearity within 2D geometry

The following examples are pertinent to optical metamaterials and devices with infinite extent along one of Cartesian coordinates, so that they can be described by a 2D cross-section geometry. Eq. (5) gives the inverted tensor $\boldsymbol{\varepsilon}^{-1}$ obtained from a known non-linear susceptibility function $\boldsymbol{\chi}$. In a centrosymmetric material, the tensor $\boldsymbol{\chi}$ can be approximated by a polynomial using even powers of $|\vec{E}|$. Thus, the lowest-order effect gives the following cubic non-linearity

$$\boldsymbol{\varepsilon} = \boldsymbol{\varepsilon}_l + \boldsymbol{\chi}^{(3)}|\vec{E}|^2. \tag{9}$$

Although a general solution of the matrix Eq. (5) can be also readily obtained, here we focus on its scalar (isotropic) version of (9) from now on using scalars, ε, ε_l, and $\chi^{(3)}$

$$\varepsilon|\varepsilon|^2 - \varepsilon_l|\varepsilon|^2 = f. \tag{10}$$

where a general case is considered, i.e., $f = 3\chi^{(3)}\omega^{-2}|\nabla h|^2 = f' + if''$, $\varepsilon = \varepsilon' + i\varepsilon''$, and $\varepsilon_l = \varepsilon_l' + i\varepsilon_l''$. We note that since

$$\varepsilon' = \varepsilon_l' + f'|\varepsilon|^{-2}, \quad \varepsilon'' = \varepsilon_l'' + f''|\varepsilon|^{-2}, \tag{11}$$

then, using substitution $\xi = |\boldsymbol{\varepsilon}|^2$, Eq. (10) can be reduced to the cubic equation with real coefficients

$$\xi^3 - a_2\xi^2 - a_1\xi - a_0 = 0. \tag{12}$$

where $a_2 = |\varepsilon_l|^2$, $a_1 = 2(\varepsilon_l' f' + \varepsilon_l'' f'')$, and $a_0 = |f|^2$. Another useful version of (12) is

$$\xi^3 - (\varepsilon_l' \xi + f')^2 - (\varepsilon_l'' \xi + f'')^2 = 0. \tag{13}$$

Since only a positive real root is of interest to us, we may use a trigonometric (or a Chebyshev cubic root) approach to the solution of (12) [6]. Thus, utilizing the substitution $\xi = 2v + \frac{1}{3}a_2$, we reduce (12) to

$$\xi^3 - p\xi = q, \tag{14}$$

with p and q being $a_1 + \frac{1}{3}a_2^2$ and $a_0 + \frac{1}{3}a_2(a_1 + \frac{2}{9}a_2^2)$, respectively.

At the singular case, $p = 0$, the solution is straightforward; or else, by taking $\xi = (2u + \frac{1}{3}a_2 v^{-1})v$, with $v = \sqrt{\frac{1}{3}|p|}$ and multiplying by $\frac{1}{3}v^{-3}$, (14) can be reduced to one of the form

$$4u^3 - sign(p)3u = \frac{1}{2}qv^{-3}. \tag{15}$$

In a passive lossy medium ($p > 0$), the solution is defined solely by the ratio $\rho = \frac{1}{2}qv^{-3}$ in the equation

$$4u^3 - 3u = \rho. \tag{16}$$

Thus, if $0 < \rho \leqslant 1$, then while solving Eq. (16) we may reverse the third-order Chebyshev polynomial of the first kind $T_3(u) = \cos(3\cos^{-1}u) = 4u^3 - 3u$, to get $\cos(3\cos^{-1}v) = \rho$ and then

$$u = \cos\left(\frac{1}{3}\cos^{-1}\rho\right). \tag{17}$$

For this case, in general the solution does not seem to be unique because v may assume three values, obtained through multiples of $2\pi/3$. In addition, the other restriction is applicable in this case ($\xi > 0$). Alternatively, if $\rho > 1$, then in solving Eq. (16), we may use the same polynomial, but now defined for $u \geqslant 1$ as $T_3(u) = \cosh(3\cosh^{-1}u) = 4u^3 - 3u$, and obtain,

$$v = \cosh\left(\frac{1}{3}\cosh^{-1}\rho\right). \tag{18}$$

We will validate our general formulation using two most frequent situations in optical metamaterials: (1) when the linear absorption of a given nanostructured elemental material is negligible, $\varepsilon_l = \varepsilon_l'$, and (2) when the elemental material is exhibiting either a purely real (lossless Kerr-type medium, $f'' = 0$) or purely imaginary (nonlinear absorber, $f' = 0$) third-order non-linearity following our earlier study [5].

4. Kerr-type medium

Here we define, $\varepsilon_l'' = 0$ and $f'' = 0$, (i.e., $\varepsilon = \varepsilon'$ and $f = f'$) and directly use (13) to obtain

$$[\varepsilon^3 - (\varepsilon_l\varepsilon^2 + f)][\varepsilon^3 + (\varepsilon_l\varepsilon^2 + f)] = 0. \tag{19}$$

We ignore the second term $\boldsymbol{\varepsilon}^3 + (\boldsymbol{\varepsilon}_l\boldsymbol{\varepsilon}^2 + f)$, thus solving only for $\boldsymbol{\varepsilon}^3 - \boldsymbol{\varepsilon}_l\boldsymbol{\varepsilon}^2 - f = 0$. Then, using $\boldsymbol{\varepsilon} = (1 + 2u)v$, $\rho = 1 + \frac{1}{2}fv^{-3}$ and $v = \boldsymbol{\varepsilon}_l/3$, we finally obtain the Chebyshev form, $4u^3 - 3u = \rho$. The real root for $\rho \geqslant 1$ is $u = \cosh\left(\frac{1}{3}\cosh^{-1}\rho\right)$, so that

$$\varepsilon = v + 2v\cosh\left(\frac{1}{3}\cosh^{-1}\rho\right) = (1 + a + a^{-1})v, \tag{20}$$

where $a = (\rho + \sqrt{\rho^2 - 1})^{1/3}$.

5. Absorption saturation effect

Suppose now that we would like to analyze the influence of the saturation effect of a certain elemental material on the overall performance of a nanostructured photonic device during intense optical field propagation. A typical example would be the study of the beam profile in a metamaterial consisting of metallic wires embedded in a non-linear absorbing host. We use a basic interpolation formula, derived for a saturable absorber, as a starting point. Recall that in a lossy medium, a finite volume cannot absorb an infinite amount of energy since only a limited number of atoms can be excited from their ground state into an excited state. Hence, the simplest description of the process related to (7) takes the interpolation form

$$\varepsilon = \varepsilon_l + i\tilde{\chi}, \tag{21}$$

where the saturable absorber part is $\tilde{\chi} = \varepsilon''/(1 + (\varepsilon''/q_{\max})|\vec{E}|^2)$, $q_{\max}$ is the maximal power absorbable per unit volume, and ε'' defines constant linear losses at low-intensity excitation. After replacing $\varepsilon_l^2 + \omega^{-2}\varepsilon''|\nabla h|^2/q_{\max}$ with τ, (21) yields a cubic-type equation with real coefficients

$$\tilde{\chi}^3 - \varepsilon''\tilde{\chi}^2 + p\tilde{\chi} - \varepsilon''\varepsilon_l^2 = 0, \tag{22}$$

which is a particular case of a general cubic non-linearity already discussed above.

After substituting into $\tilde{\chi} = 2uv + \frac{1}{3}\varepsilon''$ the relation $v = \frac{1}{3}\sqrt{|\varepsilon''^2 - 3\tau|}$, and multiplying (22) by $\frac{1}{2}v^{-3}$, the latter equation arrives at another Chebyshev form, $4u^3 - 2su = \rho$, where the sign factor is $s = sign(\varepsilon''^2 - 3\tau)$ and $\rho = \frac{1}{2}\varepsilon''(2\varepsilon''^2 - 9\tau + 27\varepsilon_l^2)/|\varepsilon''^2 - 3\tau|^{3/2}$. For $s < 0$, the only relevant root is $u = \sinh\left(\frac{1}{3}\sinh^{-1}\rho\right)$, and,

$$\begin{aligned}\varepsilon &= \varepsilon_l + i\frac{1}{3}\varepsilon'' + i2v\sinh\left(\frac{1}{3}\sinh^{-1}\rho\right)\\ &= \varepsilon_l + i\frac{1}{3}\varepsilon'' + iv(b - b^{-1}),\end{aligned} \tag{23}$$

where $b = \left(\rho + \sqrt{\rho^2 + 1}\right)^{\frac{1}{3}}$.

6. Validation test and simulation example

Validation of the FE models for the absorbing and Kerr media was performed using commercial finite element software [7]. An alternative 1D ODE solution has been used to validate both solutions, as $E_{s,H} = (|S_H - S_0|/|S_0|)100\%$ and $E_{s,E} = (|S_E - S_0|/|S_0|)100\%$ where S_H and S_E are the components of the time-averaged Poynting vector taken along the propagation direction for the H-field and E-field formulations, respectively.

6.1. Validation test: H-field versus E-field formulation (homogeneous Kerr slab)

First, S_0 is calculated through a standard technique for solving a system of ODEs [8], giving a relative error below 10^{-3}% for any given point within a 560-nm slab of a Kerr-type non-linear medium ($\boldsymbol{\varepsilon}_l = 2.25 + \imath 0$ and $\chi^{(3)} = (10^{-18} + \imath 0)\,\mathrm{m}^2/\mathrm{V}^2$). This is true for both the H-field and E-field formulations of the normally incident the 850-nm wavelength light with the magnitude of the electric field ranging from 100 to 350 MV/m. Fig. 1a depicts a color map of the relative error in the non-linear dielectric function calculated as $E_{\boldsymbol{\varepsilon}} = (|\boldsymbol{\varepsilon}_H - \boldsymbol{\varepsilon}_E|/|\boldsymbol{\varepsilon}_E|)100\%$ for the Kerr slab using an electric field magnitude of 350 MV/m; here $\boldsymbol{\varepsilon}_H$ and $\boldsymbol{\varepsilon}_E$ are the time-averaged dielectric function components taken along the incident E-field for both the H-field and E-field formulations. Fig. 1b shows the relative error of the time-averaged Poynting vector for the scalar H-mode with $\boldsymbol{\varepsilon}$ obtained from (19), while using the scalar E-mode $\boldsymbol{\varepsilon}$ obtained from (9) as a reference. The simulation results are obtained using the finite element method [7,9] built on the variational formulation of the scalar equation (6).

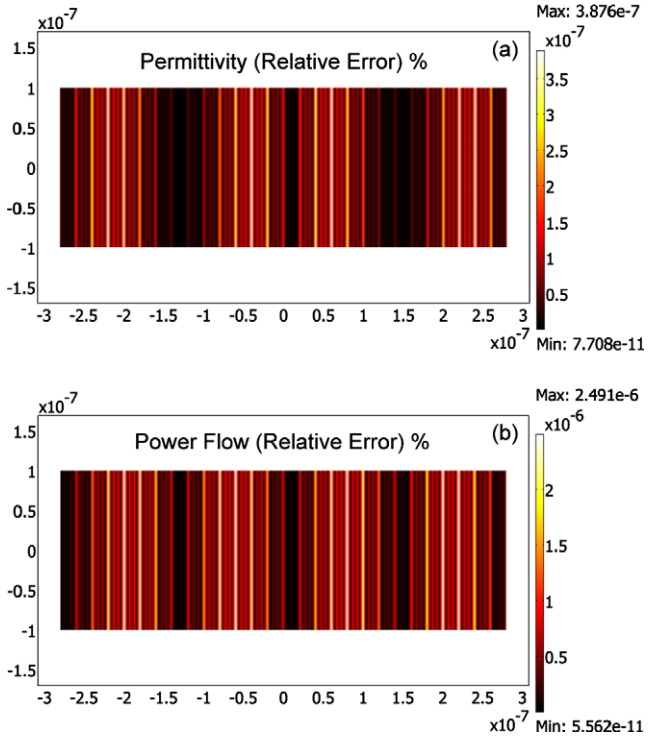

Fig. 1. Validation of the FE scalar H-field models. (a) Relative error in time-averaged ε of a 560-nm thick non-linear Kerr slab ($\varepsilon_l = 2.25$ and $\chi^{(3)} = 10^{-18}$ m^2/V^2) with effective ε obtained from (19). (b) Relative error in time-averaged power flow through the slab calculated using scalar H-field formulation with effective ε also obtained from (19).

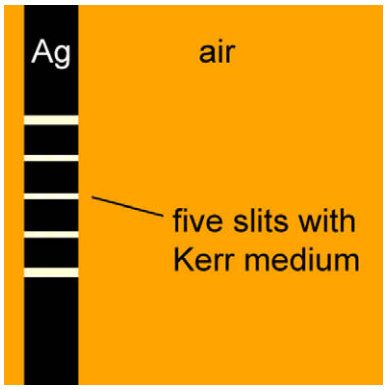

Fig. 2. Geometry of a non-linear focusing device. A 570-nm thick silver film is illuminated by 850-nm plane wave moving from left to right through five sub-wavelength slits (with 100-, 70-, 60-, 70-, 100-nm width sequence) distributed evenly from top to bottom with 400-nm offsets between their centers.

6.2. Non-linear focusing device

Fig. 2 shows the geometry of a non-linear focusing device adapted from [10]. The device is a 570-nm thick silver slab with five sub-wavelength slits (with 100-, 70-, 60-, 70-, 100-nm widths sequence) distributed evenly from top to bottom, having identical 400-nm offsets between their centers. The structure is illuminated by a 850-nm plane wave moving from left to right through the slits filled with a non-linear Kerr medium (with $\varepsilon_l = 2.25 + i0$ and $\chi^{(3)} = (10^{-18} + i0)$ m^2/V^2).

The intensity-tunable, focusing capability is enabled through the use of different surface plasmon–polariton modes excited in the structure at different intensities of the incident light. Fig. 3a–c depicts the intensity-tunable refractive index in the slits. Fig. 3a shows the distribution of the non-linear part of the refractive index $\Delta n = n - \sqrt{\varepsilon_l}$ in the slits for the incident E-field magnitude of 100 MV/m. Here the maximum of $\Delta n = 0.305$ is obtained inside the central slit, and the widest slits (100-nm slits at the top and bottom) are not activated yet. Fig. 3b shows the evolution of this process as the incident magnitude approaches 200 MV/m. The maximum of $\Delta n = 0.305$ is still achieved in the central slit, but the widest 100-nm slits are already moderately engaged. Finally, as the incident magnitude reaches 350 MV/m level, the maximum $\Delta n = 0.608$ is now obtained in the fully activated widest slits, while the central slit is almost deactivated.

The above process results in an intensity-tunable focusing performance sequentially shown in Fig. 4a–c as the intensity increases

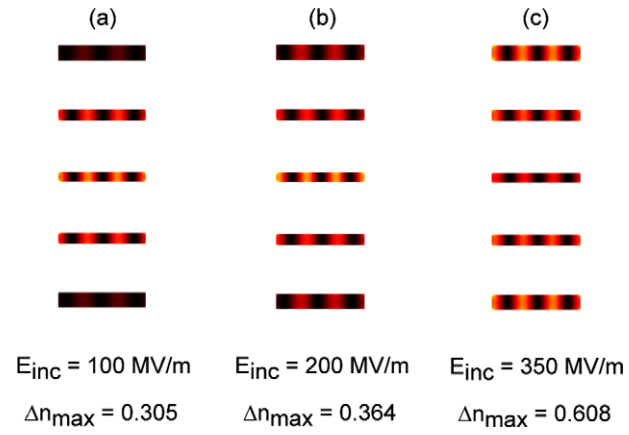

Fig. 3. Intensity-tuned refractive index in the slits of a non-linear focusing device. (a) Incident magnitude is 100 MV/m, maximal Δn of 0.305 is obtained in the central slit, while the widest slits (at the top and bottom) are not activated yet. (b) Incident magnitude is 200 MV/m, maximal Δn of 0.364 is still obtained in the central slit, but the widest slits (at the top and bottom) are already moderately engaged. (c) Incident magnitude is 350 MV/m, maximal Δn of 0.608 is now obtained in the widest slits, while the central slit is almost deactivated.

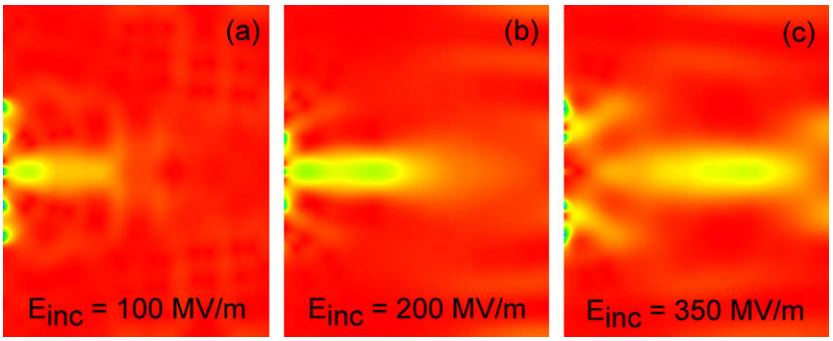

Fig. 4. Intensity-tunable focusing at the incident magnitude of 100 MV/m (a), 200 MV/m (b), and 350 MV/m (c).

from 100 to 350 MV/m. The constructive interference of the different activated slits moves the focal point further away from the device. Qualitatively, the process is similar to that described in Ref. [7].

7. Summary and conclusion

We present a set of numerical experiments demonstrating a novel approach to modeling third-order non-linear optical responses in 2D nanostructures illuminated with TM waves. The proposed method uses a problem-specific 2D non-linear material model to keep the purely scalar TM formulation and takes account of the cubic non-linearity.

The proposed approach is built on the solution of the implicit equation for the non-linear dielectric function. All important features of the method are analyzed using a general cubic non-linearity as an example. A simpler approach has been already derived and tested for the basic case of lossless linear susceptibility, and either purely real or purely imaginary cubic susceptibility [5]. The proposed general solution for scalar *H*-field waves is validated versus our previously tested cases, and important differences between those cases and the general solution are detailed. These details, for example, include the link between linear and non-linear loss mechanisms, and the connection between the linear and non-linear dielectric functions.

First, the method is successfully validated for a uniform non-linear slab solved separately with an alternative method for 1D model of lossless Kerr medium [8], and then, with a separate finite element simulation using the same mesh and geometry, but with the scalar *E*-field formulation.

Detailed simulation results are obtained for a non-linear focusing device with optically controlled isotropic Kerr-type non-linearity. To simplify the validation procedure, the device geometry and material parameters are adapted from [10], where embedding a non-linear material in the sub-wavelength slits of the thick silver film is proposed as a new method of all-optical control of the output beam. The core principles, activation of the slit polaritonic modes and consequent tunable beam focusing, are illustrated using the novel approach in FE modeling environment; the simulation results prove the predicted functioning of the device tested with our more efficient simulation approach.

The method certainly has wider application that goes beyond the third-order non-linearity in metamaterials, and can be used in the general context of solving the scalar *H*-field Eq. (6) with implicit non-linear equation (5).

This work was supported in part by ARO grants W911NF-04-1-4070350, W911NF-09-1-0075, W911NF-09-1-0231, and ARO-MURI award 50342-PH-MUR.

References

[1] G. Cevini, G. Oliveri, M. Raffetto, IET Microw. Antennas Propag. 1 (2007) 737.
[2] G. Cevini, G. Oliveri, M. Raffetto, Microw. Opt. Technol. Lett. 48 (2006) 2524.
[3] Z. Liu, A. Boltasseva, R.H. Pedersen, R. Bakker, A.V. Kildishev, V.P. Drachev, V.M. Shalaev, Metamaterials 2 (2008) 45.
[4] W. Cai, U.K. Chettiar, Y. Hsiao-Kuan, V.C. de Silva, A.V. Kildishev, V.P. Drachev, V.M. Shalaev, Opt. Exp. 15 (2007) 3333.
[5] A.V. Kildishev, Y. Sivan, N.M. Litchinitser, V.M. Shalaev, Opt. Lett. 34 (2009).
[6] G. Birkhoff, S. Mac Lane, Survey of Modern Algebra, fourth ed., Macmillan, New York, 1977. pp. 102–103.
[7] COMSOL Multiphysics, User's Manual.
[8] H.V. Baghdasaryan, T.M. Knyazyan, Opt. Quant. Electron. 31 (1999) 1059.
[9] J. Jin, The Finite Element Method in Electromagnetics, Wiley, New York, 1993.
[10] C. Min, P. Wang, X. Jiao, Y. Deng, H. Ming, Opt. Exp. 15 (2007) 9541.